

Time reversal & adjoint wavefields

ErSE390 Seismic waves

1. Time-reversal simulations
2. Adjoint method and sensitivity kernels
3. Imaging principle, reverse-time migration & seismic interferometry

The basic wave equation has a time symmetry with the equation being invariant under reversed time. This is being exploited in various ways, from time-reversal simulations and backprojections, to adjoint methods, sensitivity kernel simulations and reverse-time migration. Here, we will briefly review some of these concepts in the context of seismic ground motions to highlight their connections.

Time-reversal simulations

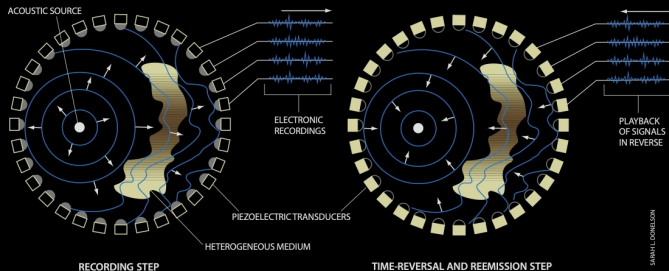
As an illustration, taking the simple 1D homogeneous acoustic wave equation

$$\frac{\partial^2}{\partial t^2} u(x, t) = c(x)^2 \frac{\partial^2}{\partial x^2} u(x, t) \quad (1)$$

where $u(x, t)$ is displacement and $c(x)$ acoustic wave speed. Replacing time t with its negative $-t$ leads to the exact same equation and $u(x, -t)$ is also a solution. That is, the wave equation is invariant under time reversal (or self-adjoint in time). This remains true no matter how complicated the medium described by $c(x)$ is.

This **time-symmetry** property of the wave equation also holds for elastic waves, but starts breaking down if attenuation, rotational or gravitational effects are included. In those cases, some of the additional equation terms will either change sign or as in case of attenuation, will need to "re-inject" energy which is an unstable procedure. A time-reversed simulation will need to account for that. For simplicity and laboratory experiments, these additional effects are often considered to be small and ignored.

Time-reversal mirror



Running wave simulations backward in time can lead to many interesting methods and applications. One of these being the time-reversal mirror concept which was experimented by [Fink, 1992, Fink, 1999] for acoustic waves.

Having a dense set of recorders and re-injecting the time-reversed records will focus the wave energy back to its original source location. A recorder array thus can act as an acoustic mirror, reflecting back waves to determine their origin.

Using numerical wave propagation solvers, this experiment can be conducted for not only acoustic but also elastic waves in a virtual setup and compared to laboratory or real-earth experiments.

Adjoint method and sensitivity kernels

The original work by [Tarantola, 1984] shows that the seismic inverse problem can be iteratively solved by numerically calculating the Fréchet derivatives (which represents the sensitivity of a seismogram with respect to the model parameters) of a waveform misfit function. The construction of these derivatives involves the interaction between the forward wavefield and a wavefield obtained by using the time-reversed differences between data and synthetics. This second wavefield is similar to the time-reversal simulation met in the previous section by backpropagating the differences injected at the receiver positions.

Later on, the concept of an "adjoint" calculation was introduced by [Talagrand and Courtier, 1987] to determine the gradient of a misfit function, Tarantola's waveform misfit being one particular example of this more general concept. Time-reversal has thus become an integral part of seismic inverse problems.

Adjoint equation of motion

Let's look at the equations of motion for elastic waves, both the forward and adjoint wavefield:

Equation of motion

$$\rho \partial_t^2 \mathbf{s} = \nabla \cdot \mathbf{T} + \mathbf{f}$$

Adjoint equation of motion

$$\rho \partial_t^2 \mathbf{s}^\dagger = \nabla \cdot \mathbf{T}^\dagger + \mathbf{f}^\dagger$$

The equation of motion is self-adjoint, and thus the same wave propagation solver can be used to compute the forward wavefield \mathbf{s} and adjoint wavefield \mathbf{s}^\dagger . In the adjoint case, the simulation just runs backward in time using an adjoint source \mathbf{f}^\dagger .

The choice of misfit to measure the difference between synthetic and observed receiver traces, e.g., a waveform misfit:

$$\chi(\mathbf{m}) = \frac{1}{2} \sum_{r=1}^{N_r} \int_0^T \omega_r(t) \|\mathbf{s}(\mathbf{x}_r, t; \mathbf{m}) - \mathbf{d}(\mathbf{x}_r, t)\|^2 dt$$

determines the adjoint source

$$\mathbf{f}^\dagger(\mathbf{x}, t) = \sum_{r=1}^{N_r} \omega_r(t) [\mathbf{s}(\mathbf{x}_r, T - t) - \mathbf{d}(\mathbf{x}_r, T - t)] \delta(\mathbf{x} - \mathbf{x}_r)$$

Following [Tromp et al., 2005], the total misfit change for a model parameterization with density ρ , shear μ and bulk κ modulus can be written as

$$\delta\chi = \int_V [K_\rho(\mathbf{x}) \delta \ln \rho(\mathbf{x}) + K_\mu(\mathbf{x}) \delta \ln \mu(\mathbf{x}) + K_\kappa(\mathbf{x}) \delta \ln \kappa(\mathbf{x})] d^3\mathbf{x}$$

with the sensitivity kernels

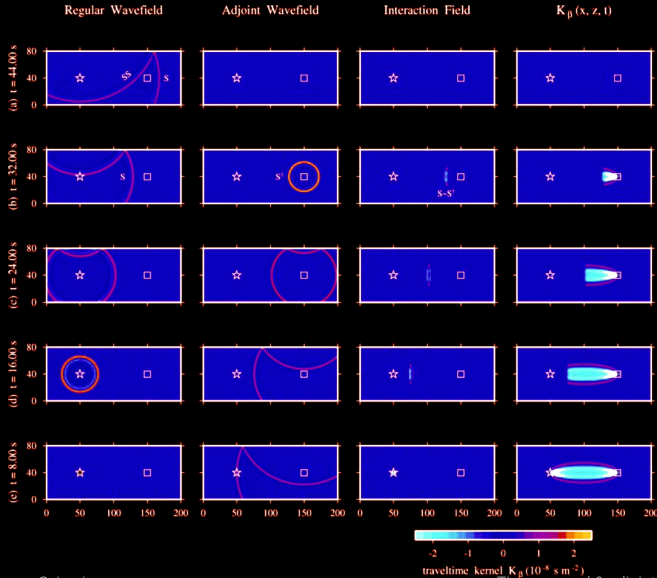
$$K_\rho(\mathbf{x}) = - \int_0^T \rho(\mathbf{x}) \partial_t \mathbf{s}^\dagger(\mathbf{x}, T-t) \cdot \partial_t \mathbf{s}(\mathbf{x}, t) dt$$

$$K_\mu(\mathbf{x}) = - \int_0^T 2\mu(\mathbf{x}) \mathbf{D}^\dagger(\mathbf{x}, T-t) : \mathbf{D}(\mathbf{x}, t) dt$$

$$K_\kappa(\mathbf{x}) = - \int_0^T \kappa(\mathbf{x}) [\nabla \cdot \mathbf{s}^\dagger(\mathbf{x}, T-t)] [\nabla \cdot \mathbf{s}(\mathbf{x}, t)] dt$$

where $\mathbf{D} = \frac{1}{2}[\nabla \mathbf{s} + (\nabla \mathbf{s})^T] - \frac{1}{3}(\nabla \cdot \mathbf{s})\mathbf{I}$ (and \mathbf{D}^\dagger) is the traceless (adjoint) strain deviator.

Adjoint sensitivity kernels II

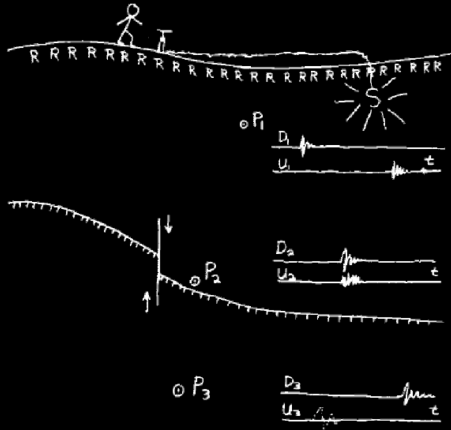


Note how the sensitivity kernel expressions are cross-correlations in time of a forward and adjoint (backward in time) wavefield expression, calculated at every position of the subsurface model.

The interaction contribution at every time step thus requires having the forward wavefield at time t and the adjoint wavefield at time $T - t$ readily available.

Imaging principle, reverse-time migration & seismic interferometry

Imaging principle I



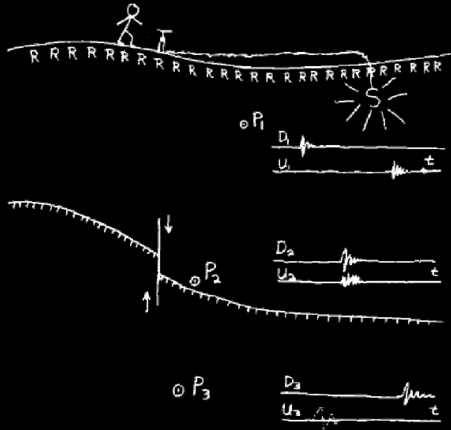
from Claerbout, 1971

According to [Claerbout, 1971]'s imaging principle, the reflector position is determined by the time and space where the source wavefield $u(x, z, t)$ and the receiver wavefields $r(x, z, t)$ coincide:

$$I(x, z) = \frac{u(x, z, t_d)}{r(x, z, t_d)} \quad (2)$$

where $I(x, z)$ is the reflectivity strength. The time t_d is a priori unknown.

A practical way to compute the reflector strength and position is to assume it to be at the zero lag of the cross-correlation between source and receiver wavefields in time.

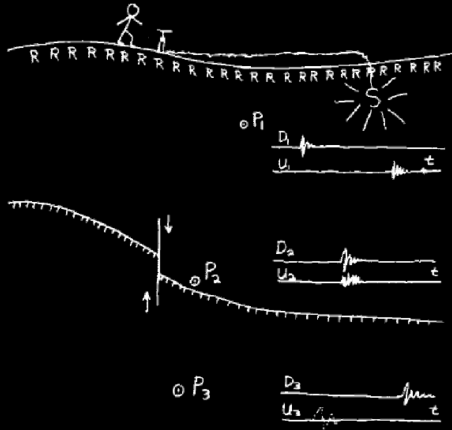


from Claerbout, 1971

This imaging principle is related to the adjoint sensitivity kernels we met before. As an example, setting in the imaging principle the source wavefield $u(\mathbf{x}, t) = \partial_t s(\mathbf{x}, t)$ and receiver wavefield $r(\mathbf{x}, t) = \partial_t s^\dagger(\mathbf{x}, T - t)$ we find:

$$\begin{aligned}
 I(\mathbf{x}) &= \frac{u(\mathbf{x}, t_d)}{r(\mathbf{x}, t_d)} \\
 &\approx \frac{\int_0^T u(\mathbf{x}, t) r(\mathbf{x}, t) dt}{\int_0^T r^2(\mathbf{x}, t) dt} \\
 &\sim \int_0^T \partial_t s(\mathbf{x}, t) \cdot \partial_t s^\dagger(\mathbf{x}, T - t) dt \\
 &\sim K_\rho(\mathbf{x})
 \end{aligned}$$

Imaging principle III

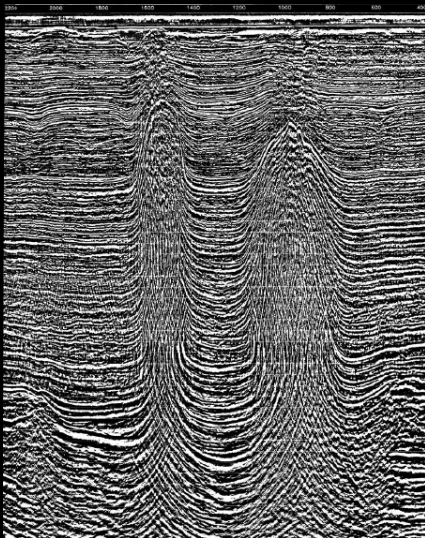


from Claerbout, 1971

Similar in elastic imaging, where for example a P-to-P imaging principle is related to the bulk sensitivity kernel expression [Zhu et al., 2009]:

$$\begin{aligned}
 I_{PP}(\mathbf{x}) &= \int_0^T [\nabla \cdot \mathbf{u}(\mathbf{x}, t)][\nabla \cdot \mathbf{r}(\mathbf{x}, t)] dt \\
 &= \int_0^T [\nabla \cdot \mathbf{s}(\mathbf{x}, t)][\nabla \cdot \mathbf{s}^\dagger(\mathbf{x}, T - t)] dt \\
 &\sim K_\kappa(\mathbf{x})
 \end{aligned}$$

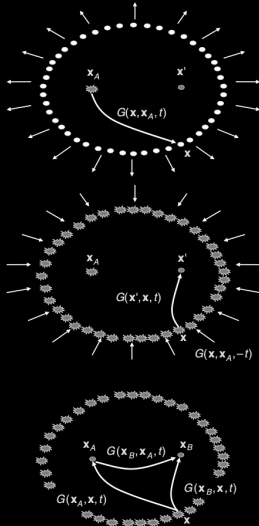
Reverse-time migration



In reverse-time migration, the main principle relies on re-injecting the reversed, recorded wavefield at the receivers and backpropagate it into the subsurface. There are 3 steps involved to obtain a reverse-time migration image:

1. for a single shot, forward propagate the source wavefield,
2. re-inject the recorded wavefield and backpropagate the recorder wavefield,
3. apply an imaging condition, e.g., the one from Claerbout.

Stack all the images from all preferred shots together (possibly processed to suppress noise) to get the final RTM image of the subsurface. Note that the velocity model is kept fixed and identical for all the modeling.



The time-reversal mirror concept seen before can also be used to explain the underlying theory of seismic interferometry (see, e.g., [Wapenaar et al., 2010]).

The cross-correlation between two traces recorded at receiver positions \mathbf{x}_A and \mathbf{x}_B to retrieve the Green's function $G(\mathbf{x}_B, \mathbf{x}_A, t)$ can be seen as the cross-correlation of the forward wavefield emitted by an impulsive source at position \mathbf{x}_A and a time-reversed wavefield captured at position \mathbf{x}_B .

An excellent overview on time-reversal in seismology is given by [Larmat and Clay, 2019].

More details can be found for example in:



Claerbout, J. F. (1971).

Toward a unified theory of reflector mapping.

Geophysics, 36(3).



Fink, M. (1992).

Time reversal of ultrasonic fields - part I: Basic principles.





IEEE Transactions on ultrasonics, ferroelectrics, and frequency control, 39(5).





Fink, M. (1999).

Time-reversed acoustics.

Scientific American, 281(5):91–97.

-  Larmat, C. and Clay, C. S. (2019).
Time-reversal in seismology.
In Gupta, H. K., editor, *Encyclopedia of Solid Earth Geophysics*, Encyclopedia of Earth Sciences Series. Springer Nature Switzerland.
-  Talagrand, O. and Courtier, P. (1987).
Variational assimilation of meteorological observations with the adjoint vorticity equation. i: Theory.
Meteorol. Soc., 113:1311–1328.
-  Tarantola, A. (1984).
Inversion of seismic reflection data in the acoustic approximation.
Geophysics, 49(8).
-  Tromp, J., Tape, C., and Liu, Q. (2005).
Seismic tomography, adjoint methods, time reversal and banana-doughnut kernels.
Geophys. J. Int., 160(1):195–216.

-  Wapenaar, K., Slob, E., Snieder, R., and Curtis, A. (2010).
Tutorial on seismic interferometry: Part 2 - underlying theory and new advances.
Geophysics, 75(5).
-  Zhu, H., Luo, Y., Nissen-Meyer, T., Morency, C., and Tromp, J. (2009).
Elastic imaging and time-lapse migration based on adjoint methods.
Geophysics, 74(6).